Physics of the Solid State, 2025, Vol. 67, No. 7

02,08

Features of resistance, critical temperature and microstructure of cryogenic thin aluminum films

© M.A. Tarasov[1], A.A. Lomov[2], K.D. Shcherbachev[3], A.A. Tatarintsev[2], M.V. Strelkov[1], D.S. Zhogov[1], R.K. Kozulin[1], A.M. Chekushkin[1], M.A. Markina[1,4], A.D. Golovanova[4,5], A.M. Troyanovsky[5], A.L. Vasiliev[6,7]

[1] Kotelnikov Institute of Radio Engineering and Electronics, Russian Academy of Sciences,
Moscow, Russia
[2] Department of Valiev Institute of Physics and Technology,
Research and Engineering Center „Kurchatov Institute",
Moscow, Russia
[3] National University of Science and Technology MISiS,
Moscow, Russia
[4] National Research University Higher School of Economics,
Moscow, Russia
[5] Kapitza Institute for Physical Problems, Russian Academy of Sciences,
Moscow, Russia
[6] Department of „Shubnikov Crystallography Institute of „Kurchatov Complex of Crystallography and Photonics" (KCCP),
Research and Engineering Center „Kurchatov Institute",
Moscow, Russia
[7] Moscow Institute of Physics and Technology (National Research University),
Dolgoprudny, Moscow Region, Russia

E-mail: tarasov@hitech.cplire.ru

Received March 6, 2025
Revised March 6, 2025
Accepted May 5, 2025

Aluminum films with a thickness of 120 nm and multilayer structures based on them were fabricated by the vacuum thermal evaporation method and experimentally studied. Unlike bulk samples, they demonstrated an order of magnitude higher resistivity up to $260\,\Omega\cdot$nm and a doubled superconducting transition temperature of 2.3 K. It was shown that the observed features are due to both the chemical activity of aluminum and a decrease in the crystallite growth rate. It was found that when evaporating onto a Si(111) substrate cooled with liquid nitrogen, a decrease in the crystallite grain size from 50 nm to 15 nm and a decrease in the surface roughness to rms about 1 nm are observed. The measured transport properties of the studied cryogenic aluminum structures are associated with a decrease in the film thickness and the mean free path of electrons, the appearance of additional scattering of current carriers on oxide atoms, crystallite boundaries, structural defects, distortions and roughness of external and internal boundaries. The studies of films by AFM, SEM, STEM, EDXS, and X-ray diffraction methods showed a correlation between the microstructure and electrical parameters of the films.

Keywords: thin films, crystalline structure, surface morphology, residual resistance, kinetic inductance.

DOI: 10.61011/PSS.2025.07.61877.18HH-25

1. Introduction

The progress of the high frequency superconductor electronics is closely related to using the materials based on Al, Nb and their alloys [1]. The thin films and structures formed from them are widely used in development of superconductor microwave resonant cavities, high-sensitivity detectors based on the tunnel junctions superconductor-isolator-superconductor (SIS) [2], elements of quantum computers [3]. Electric characteristics of the films: their residual resistance and inductance, as well as mechanical and adhesion properties play an important role in expansion of the temperature range of the instruments and devices based on them. For example, this objective is achieved by a combination of the superconductor films with the normal metal film via the insulator layer in the structure (SINIS) [4]. Such a combination allows expanding the dynamic range, forming the effective electronic coolers.

Modification of the electrophysical properties of the superconducting films may be achieved using various mechanisms of their growth control or formation on different substrates. The priority objectives are the increase in the temperature of transition to the superconducting state [5] and the controlled kinetic inductance. These temperature-dependent characteristics are directly related to the microstructure and the composition of the thin films. Traditionally the metal films are grown in the form of islands using Volmer–Weber mechanism [6] by the method of thermal vacuum evaporation or magnetron sputtering [7]. To obtain the single-crystal films, mainly molecular beam epitaxy is applied. When the aluminum films are formed, they may be additionally doped with

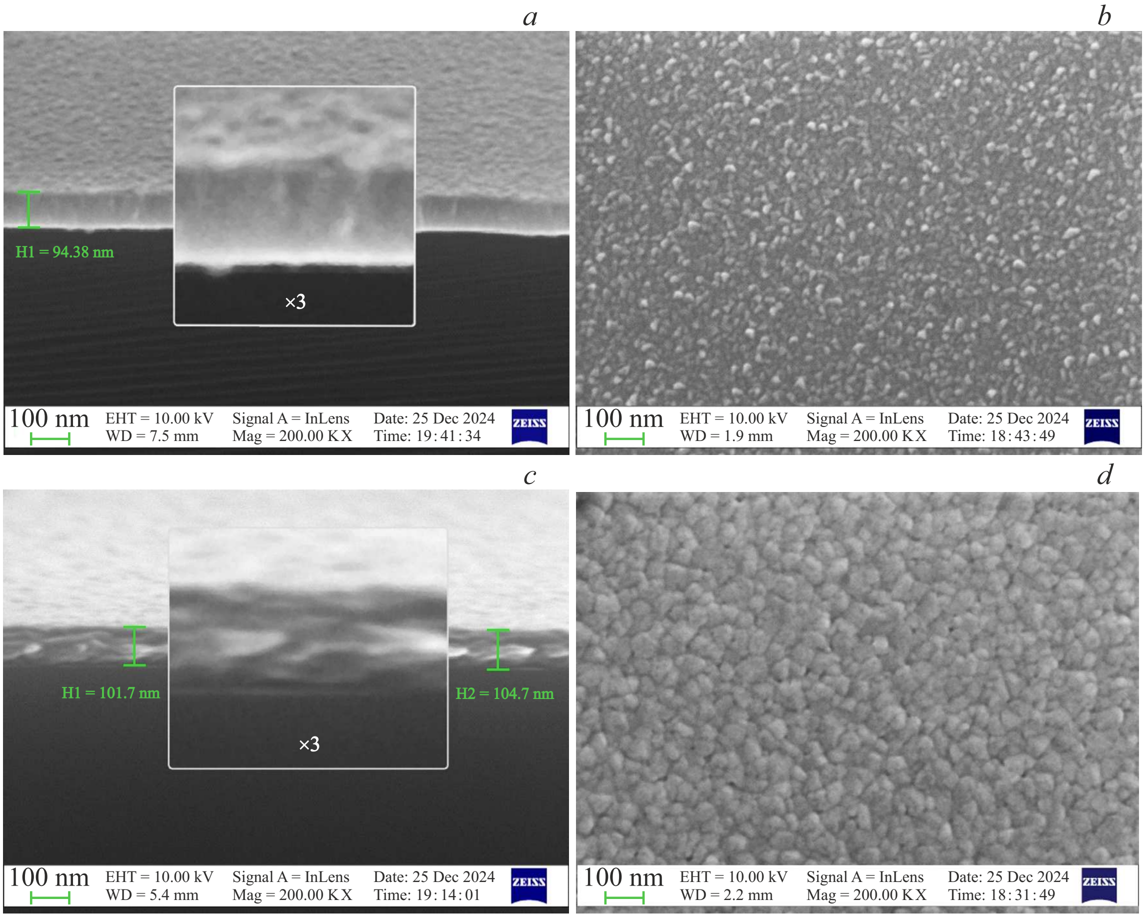

Figure 1. SEM-images of clefts (a, c) and surface (b, d) of the films sputtered at 77 and at 300 K onto the single crystal silicon substrates (111).

oxygen under thermal deposition, are alloyed with silicon and boron under magnetron sputtering in nitrogen atmosphere. In the mode of double-stage growth of the films due to the formation of the transition homobuffer layers on the substrate surface, the control of their microstructure, morphology and roughness of the surface is achieved with the same growth method [9]. The root mean square roughness (rms) of the film surface in magnetron sputtering is usually at least 5−6 nm [8]. Upon thermal evaporation the roughness value rms $\sim$ 1 nm [9] may be achieved by formation of the film on the substrates cooled down to temperatures of 77 K. The growth of the thin films of superconductors Sn, In, Al, Pb at cryogenic temperatures demonstrated significant (up to 2 times and more) increase of the superconducting transition temperature [10]. The study of such cryogenic films is usually limited to the measurement of their electrophysical characteristics without any connection to their real structure. This circumstance prevents targeted control of the growth processes in the superconducting thin films with the purpose to create multilayer heterostructures with the specified properties.

In the presented paper the method of high vacuum thermal evaporation grew the thin Al films and SIS structure on the Si(111) substrate at 77 K, and the studies of their structural features were conducted by the methods of X-ray diffractometry and reflectometry (GIXRD, XRR), methods of transmission/scanning electron microscopy (TEM/STEM), energy-dispersive X-ray spectroscopy (EDXS), and methods of scanning electron (SEM) and atomic force (AFM) microscopy. The measurements were made for the temperature dependences of resistance, the temperatures of the superconducting transition were determined, and the analysis of the connection between the electrical parameters of the films and their structural characteristics was conducted.

2. Experiment

One of the objectives of our study is to optimize the formation of thin Al films to reduce the possible leaks in SIS and SIN junctions, to increase the current density and to decrease the specific capacity by decrease of the film roughness and granularity. Figures 1−3 presents the results of the study of aluminum structures obtained with the help of the electronic microscope made by vacuum

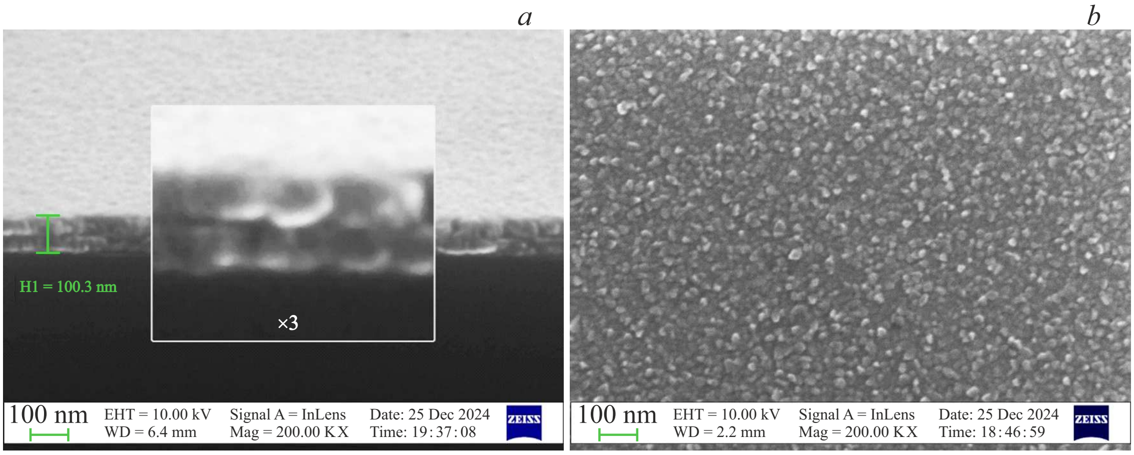

Figure 2. SEM-images of the chip (*a*) and surface (*b*) of the aluminum SIS junction formed at 77 K. The insert with magnification of $\times 3$ shows clearly the dark dielectric layer.

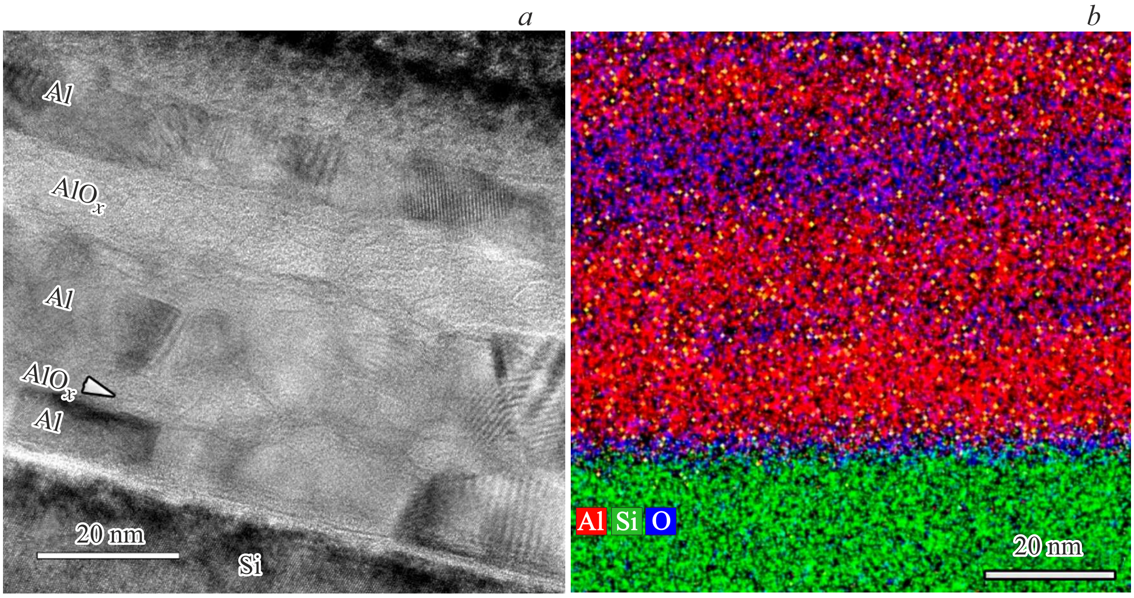

Figure 3. TEM (*a*) and EDXS (*b*) elemental mapping of the 3-layer structure obtained by vacuum sputtering with the stops of Al sublayers at 77 K.

thermal evaporation onto „hot“ at 300 K and „cryogenic“ at 77 K Si(111) substrates. The scanning electron microscope Carl Zeiss Ultra 55 was used to conduct the studies of the film topography, and to research the sample clefts. SEM-images (Figure 1) shows that the size of the grains on the surface of the cryogenic Al film (growth on the cold substrate) is 10–20 nm (Figure 1, *a, b*), the growth at room temperature forms the grains of ~ 50 nm (Figure 1, *c, d*). The grain fineness and homogeneity of the cryogenic film compared to that grown at 300 K is well-visible when the images of their clefts are compared (Figure 1, *a* and 1, *c*, accordingly).

The residual pressure of gases in the evaporation chamber makes it possible to both change the composition of the films [11] and create the multi-layer structures. The studies of the multi-layer structures were conducted by the methods of transmission/scanning electron microscopy (TEM/STEM) and energy-dispersive X-ray spectroscopy (EDXS) using a transmission/scanning electron microscope Osiris (Thermo Fisher Scientific, USA), equipped with EDXS SuperX (Bruker, Germany), at accelerating voltage of 200 kV. The cross sections of the samples were prepared by the method of the focused ion beam (FIB) using the standard method „lift-out“ in the two-beam electron ion microscope Scios (Thermo Fisher Scientific, USA). Figure 3, *a* presents the TEM-image of the 3-layer Al film on Si(111), produced in process of the growth at 77 K and with the stops between the sublayers at residual vacuum of $5 \cdot 10^{-6}$ mbar. Elemental

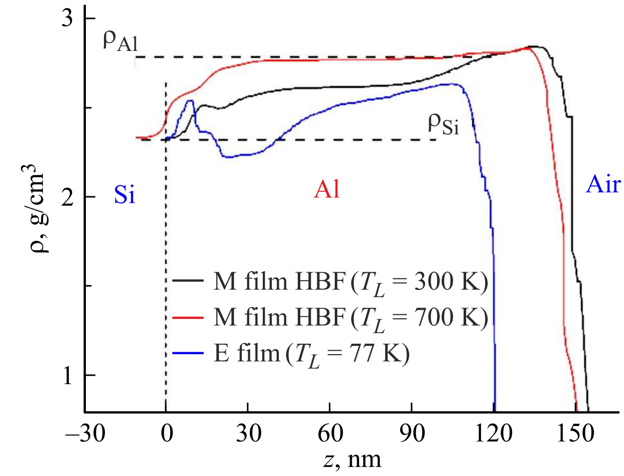

Figure 4. Densities of aluminum films evaporated on the room, hot, cold substrates.

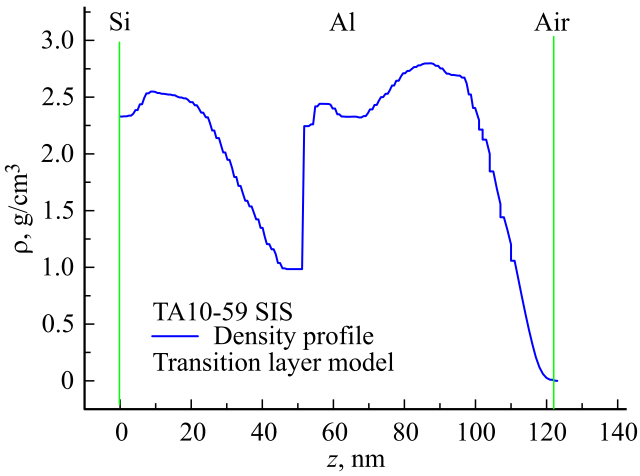

Figure 5. Density thickness profile of SIS structure evaporated on the cold substrate, in the middle lowers down to 1 g/cm^3 in the area of the oxide barrier. (the figure is adjusted).

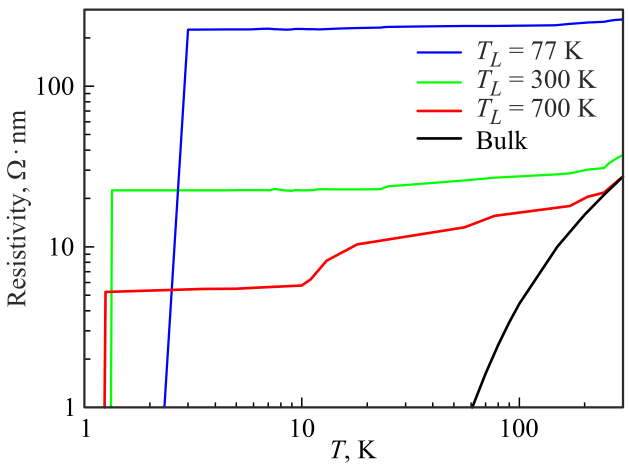

Figure 6. Specific resistance of the films deposited on the substrates having different temperature (77, 300 and 700 K), and also the annealed volume sample of pure aluminum (bulk) [12].

EDXS mapping (Figure 3, *b*) demonstrates three Al layers (shown in red) with interlayers AlO_x (shown in blue).

Films deposited onto hot substrates have a larger grain size and higher density, which is practically constant in thickness, contrary to the films on the cold substrate with smaller grains, lower density being less even in thickness (Figures 4, 5). Layer-by-layer depositing with pauses of 10–20 seconds makes it possible to obtain less stressed and less deformed films.

All the listed structural features of cryogenic films are directly reflected in the temperature dependences of resistance for different manufacturing methods given in Figure 6. The lowest specific resistance 27 Ω · nm at room temperature is that of massive aluminum, which has the practically linear dependence of resistance on temperature. And the highest specific resistance at room temperature 260 Ω · nm is in the film evaporated at 77 K, which practically does not change up to the temperature of the superconducting transition 2.3 K, which is nearly twice higher than for the volume sample $T_c = 1.18$ K.

3. Discussion of the results

According to the previous studies, the effective surface area of the aluminum SIS junction will not exceed 10 % of the geometric surface area of the structure [13]. Let us attempt to connect the effective surface area of the tunnel junction and the structure of the tunnel barrier surface. One may assume that the main areas of the tunnel conductivity in the rough film are formed on the faces and peaks of the crystallites on the film surface. At the specific value of the specific resistance of the tunnel junction 1 k Ω · μm^2 for the value of the resistance quantum $R_k = h/e^2 = 25.8\,\mathrm{k}\Omega$ we will get 26 quantum point contacts, i. e. the location of the contacts in the form of a grating 5×5 at the distance of the order of 200 μm from each other. Here there is a certain contradiction in the applied terminology, when they say pinholes [13], usually short-circuiting microcontacts are usually meant with the direct (non-tunneling) nature of conductivity, whereas in our interpretation this means the presence of a certain number of areas with higher transparency of the tunnel barrier that define the transport properties of the junction. Other areas of the junction have low transparency, make small contribution to conductivity, and their contribution to the capacitance becomes comparable to the areas of high transparency, since the capacitance linearly depends on the barrier thickness, whereas the conductivity has exponential dependence. The contribution to the critical current from each channel may be estimated as $I_n = (e^2/2h)V_\Delta T_n$, where T_n is the transparency of each channel [14]. If a less rough fine crystalline film is implemented, you may expect the increase in the number of conductivity channels, increase of the critical current, decrease in resistance and capacitance parameter ωRC.

As for the estimates of the residual specific resistance of the films, several models may be considered here. In the simplest Andrews model [15] the specific resistance $\omega_T = \omega_0 + A_T/d$ is inversely proportional to the size of the crystallite d and is directly proportional to the temperature-dependent Andrews coefficient (AT).

In the Mayadas-Schatzkes model [16], the reflection coefficient from the intergrain boundary $R$is used additionally. The dependence of the inverse specific resistance $\rho_0/\rho_{ms} = 1 - 1.5\alpha + 3\alpha^2$, where $\alpha = (l_0/d)(R/(1-R))$. For aluminum it is usually assumed that $R = 0.7-0.9$ depends on the crystallite orientation. The films with higher resistivity will have higher kinetic inductance, which can be described by a simple formula for kinetic inductance per square of film [17]

$$L_k = \hbar R_n/(\pi\Delta_0) = \hbar R_n/(1.76\pi k T_c),$$

where R_n — resistance per square of film, Δ_0 — energy gap. In this case, a significant increase in the kinetic inductance L_k can be obtained without the need to form very thin films of less than 5 nm. In our case, an increase in resistance by almost an order of magnitude and $T_c$twice would be equivalent to a 20-fold decrease in thickness, i. e., a 100 nm film would have the kinetic inductance as a 5 nm film. For comparison, let us compare to the NbTiN film of 10 nm $L_k = 25$ pH/sq, our aluminum of 100 nm 2.7 pH/sq and 10 nm 27 pH/sq, i. e. the comparable parameters may be implemented using the aluminum technology that is compatible to the one used to create qubits and quantum computers. The literature data on the deposition onto the cold substrate turn out to be poorly compatible to our presented results, since the substrates were either cooled down by the vapors of liquid nitrogen and stayed at temperatures of above 100 K, or were deposited onto the substrates cooled with liquid helium, measured at the same 4.2 K and irreversibly recrystallized (annealed) when heated to room temperature, and lost both the high specific resistance and high temperature of the superconducting junction.

4. Conclusion

Previously it was shown that the prior formation of magnetron sputtered island homobuffer layers (HBL) at the boundary with the substrate with thickness of 20−40 nm makes it possible to control the microstructure of thin homobuffer films (HBF) and their mechanical properties. The conducted studies of the film structure by AFM, SEM, TEM, EDXS, XRD and XRR methods demonstrate the correlation of the microstructure and electrical characteristics of Al films grown under different conditions. It is shown that the magnetron 150 nm Al/Si(111) film with the homobuffer layer (growth at $T_L = 700$ K), consisting of the homogeneously densely packed grains-crystallites has the constant density along the thickness. For comparison, the profile of the density distribution in thickness is given for the Al film HBF-300 formed at 300 K. The combined analysis of the obtained data shows that the decrease in the number of intergrain boundaries in the volume of HBF-700 film causes its resistance at room temperature to be close to the electrical resistance of the massive sample and the minimum values for the studied films. The alternative option is presented by cryogenic films. Upon layer-by-layer deposition onto the Si substrate cooled down to 77 K, the residual resistance R_0 and temperature of the superconducting junction T_c increase substantially, despite the decrease in the surface roughness down to 0.5−1 nm. The size of the crystallites (grains) in the films varies from 15 to 140 nm for high-resistance and the lowest resistance, accordingly. The described technology is intended to improve the characteristics of SIS and SIN junctions, to increase the operating frequencies of the devices on their basis. High-resistance aluminum films may find application for development of resonant cavities, parametric traveling-wave amplifiers, detectors on kinetic inductance and other high-sensitivity microwave devices. To form the tunnel junctions, the technology of quasi-epitaxial films growth on the hot islands may become preferable, whereas for the devices with kinetic productivity — evaporation on the cooled substrates.

Acknowledgments

The samples were made using the equipment of the Unique Research Facility „Kriointegral“ supported within the state assignment of Kotelnikov Institute of Radio Engineering and Electronics RAS. The authors would like to thank Makar Vladimirovich Chekushin for his assistance in the equipment repair.

Funding

The study was supported by the grant of the Russian Science Foundation No. 23-79-00022 (https://rscf.ru/project/23-79-00022/.

Conflict of interest

The authors declare no conflict of interest.

References

[1] A. Braginski. J. Supercond. Nov. Magn. **32**, 23−44 (2019). DOI: 10.1007/s10948-018-4884-4
[2] J. Zmuidzinas, A. Karpov, D. Miller, F. Rice, H. Leduc, J. Pearson, J. Stern. In Far-IR, Sub-mm and MM Detector Technology Workshop (2002, April).
[3] T. Ladd, F. Jelezko, R. Laflamme, Y. Nakamura, C. Monroe, J. O'Brien. Nature **464**, 45−53 (2010).
[4] M. Tarasov, A. Gunbina, A. Chekushkin, R. Yusupov, V. Edelman, V. Koshelets. Appl. Sci. **12**, *20*, 10525 (2022).
[5] M. Tarasov, L. Kuzmin, N. Kaurova. Instrum. Exp. Tech. **52**, 877−881 (2009). DOI: 10.1134/S0020441209060220.
[6] N. Kaiser. Appl. Opt. **41**, *16*, 3053−3060 (2002).

[7] M. Ohring. The Material Science of Thin Films. Academic Press, San Diego, Calif., USA (1992).
[8] A. Lomov, D. Zakharov, M. Tarasov, A. Chekushkin, A. Tatarintsev, D. Kiselev, T. Ilyina, A. Seleznev. Techn. Phys. **69**, *6*, 1636–1645 (2024). DOI: 10.1134/S1063784224060239
[9] M. Strelkov, A. Chekushkin, M. Fominsky, R. Kozulin, S. Kraevsky, A. Tatarintsev, D. Zakharov, A. Lomov, M. Tarasov. Phys. Solid State **66**, *7*, 1006–1008 (2024). DOI: 10.61011/PSS.2024.07.58966.35HH
[10] W. Buckel. Physica **126B**, 1–7 (1984).
[11] K. Okura, V.G. Lifshits, A.A. Saranin, A.V. Zotov, M. Katayama. Vvedenie v fiziku poverkhnosti (2 glava str. 46). Nauka, M. (2006). 490 s. ISBN 5-02-034355-2. (in Russian).
[12] P. D'esai, H. James, C. Ho. J. Phys. Chem. Ref. Data **13**, 1131 (1984).
[13] T. Greibe, M. Stenberg, C. Wilson, T. Bauch, V. Shumeiko, P. Delsing. Phys. Rev. Lett. **106**, 097001 (2011).
[14] D. Willsch, D. Rieger, P. Winkel, et al. Nat. Phys. **20**, 815–821 (2024). DOI: 10.1038/s41567-024-02400-8.
[15] P.V. Andrews, M.B. West, C.R. Robeson. Phil. Mag. **19**, *161*, 887–898 (1968). https://doi.org/10.1080/14786436908225855
[16] A.F. Mayadas, M. Shatzkes. Phys. Rev. B **1**, 1382 (1970).
[17] S. Doyle. Lumped Element Kinetic Inductance Detectors. PhD thesis (University of Car-diff, 2008).

Translated by M.Verenikina